Influence of Geometry and Angular Velocity on Performance of a Rotating Disk Filter

Roger Bouzerar, Michel Y. Jaffrin, Luhui Ding, and Patrick Paullier
Dept. of Biological Engineering, Technological University of Compiegne, BP 20529, 60205 Compiegne, France

The influence of internal geometry and angular velocity on the performance of a rotating-disk filtration device is described. This module consists of a disk rotating at speeds up to 2,000 rpm inside a cylindrical housing equipped with a fixed flat membrane. The test fluid was a calcium carbonate suspension (4.7-μm mean particle diameter), and the membranes were in nylon (0.2-μm mean pore diameter) and PVDF (0.1 and 0.18 μm). The shear stress on the stationary membrane in the laminar boundary-layer regime was estimated from a similarity solution, and in the turbulent regime from the friction coefficient for a flat plate. Several inlet and outlet configurations were tested. The permeate flux was independent of the axial gap (disk to membrane), but increased when the radial gap (from disk to housing) was raised from 2 to 5 mm. The inviscid fluid core in the axial gap was observed to rotate at 42% of angular velocity with a smooth disk. This factor rose to 64% when the disk was equipped with small vanes. Fouling was limited to the central part of the membrane at 1,500 rpm and disappeared completely for a disk equipped with vanes. Permeate fluxes were consistently much higher than in classic cross-flow filtration.

Introduction

In conventional cross-flow filtration, high fluid velocities are generally necessary to limit the growth of a cake on the membrane. These high velocities require energy and produce large pressure drops along the membrane. Consequently, the transmembrane pressure (TMP) remains high along most of the membrane, and this may limit solute transmission into the permeate when the cake layer on the membrane is compressible and is packed by the pressure. Dynamic filtration, which consists of creating relative motion between the membrane and its housing avoids this problem, since the high shear rates produced by the relative motion are independent of the feed flow, which can be kept low. Two different geometries have been used in commercially available devices. The first is the cylindrical Couette flow (Lopez-Leiva, 1980; Beaudoin and Jaffrin, 1989), in which the membrane is mounted on a cylinder that rotates inside a concentric one, generating Taylor vortices that further enhance the shear rates. The second geometry consists of rotating a disk between two circular fixed membranes mounted on the housing (Nuortila-Jokinen and Nyström, 1996). Such rotating-disk devices have been shown to be very effective for solute recovery from microbial suspensions, which requires that filtration be done at a low TMP (Frenander and Jönsson, 1995; Meyer et al., 1998; Pessoa and Vitolo, 1998). For instance, Harscoat et al. (1999), in our laboratory, obtained polysaccharide mass fluxes in the permeate of 0.275 $kg \cdot m^{-2} \cdot h^{-1}$ instead of 0.02 $kg \cdot m^{-2} \cdot h^{-1}$ in conventional filtration through ceramic membranes. A similar approach, used by ABB Flootek, Sweden, consists of using a rotor blade rather than a disk. Jönsson (1993) filtered a bleach plant effluent with a unit equipped with a rectangular rotor blade 287 mm long and 60 mm wide, rotating between two membranes of 0.05 m^2 area at speeds up to 900 rpm. She observed that the initial flux decreased almost linearly with rotation speed when it was decreased, but, when a cake was formed at low speed, increasing rotation speed improved the flux only marginally, indicating that the cake was only partially reversible.

Correspondence concerning this article should be addressed to M. Y. Jaffrin.

Existing Rotating Disk Systems

The CROT system (Raisio-Flootek, Finland) is multistage with 50-cm-diameter disks for a total membrane area up to 20 m^2. A pilot unit with a 1.75-m^2 cellulosic ultrafiltration membrane was used by Nuortila-Jokinen and Nyström (1996) for concentrating paper-mill effluents. Permeate fluxes at a rotor-tip azimuthal velocity of 13 m/s were higher than in conventional cross-flow filtration.

In the Spintek ST II module (Spintek, Huntington Beach, CA), the membranes are placed on the rotor, reaching an azimuthal velocity of 20 m/s at the tip. This unit has been used for concentrating nuclear wastes of low radioactivity and for microfiltration of milk. The filtration of oil–water microemulsions with a 500-cm^2 membrane-area module was reported by Dal-Cin et al. (1998). Fluid inlet and outlet are located on the back plate (on the shaft side) and the front plate, respectively, while permeate was collected through a hollow shaft. For a rotating membrane, the permeate pressure increases toward the periphery due to centrifugal forces, the effective TMP is reduced, and the flux reaches a maximum at a speed of 1,000 rpm, which was below the maximum speed used in the test.

The DMF module (Pall Corp., NY) consists of several disks mounted on the same shaft, each one rotating between two annular membranes. Fluid enters through the hollow shaft and exits through the front plate opposite to the shaft. The azimuthal velocity at the disk tip is 20 m/s for a rotation speed of 3,450 rpm. A small-scale laboratory module with a single membrane of 135 cm^2 equipped with a 0.2-μm nylon membrane was used by Frenander and Jönsson (1996) for protein separation, and by Lee et al. (1995) for the filtration of recombinant yeast cells. Permeate fluxes and solute transmission obtained by these authors were significantly higher than with conventional cross-flow filtration.

Since we were interested in extracting exopolysaccharides from fermentation broths and in concentrating hydroxide ferric suspensions in a saline medium, representative of certain nuclear effluents, in our laboratory, we undertook the construction of several rotating-disk filtration modules. This article describes the conception of such modules, designed and built in our laboratory, and the results of our investigation on the influence of internal geometry, rotation speed, and TMP

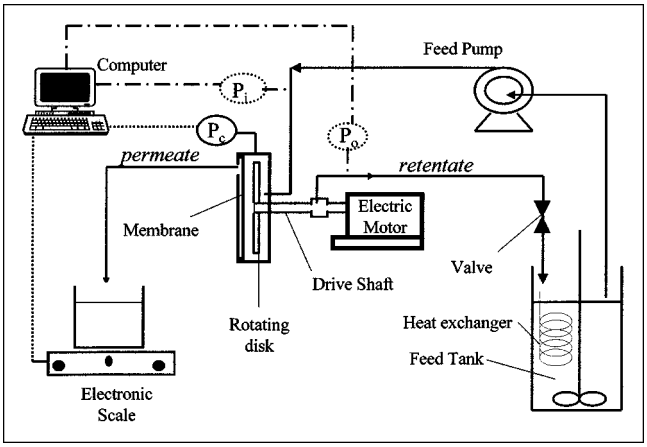

Figure 1. Experimental setup.

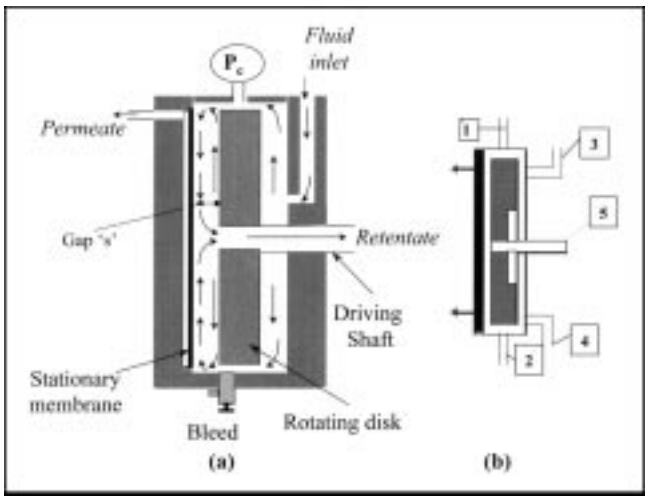

Figure 2. (a) Rotating disk module showing internal circulation; (b) inlet and outlet configurations.

on the microfiltration of $CaCO_3$ particulate suspensions selected as a test fluid due to their good reproducibility.

Material and Methods

Filtration test bench

The filtration test bench is shown in Figure 1. The filtration module was fed from a thermostated and stirred 10-L reservoir by a peristaltic pump (Masterflex, maximum flowrate of 1.7 L/min), and the collected permeate was weighed continuously by an electronic scale connected to a microcomputer in order to determine the permeate flowrate. The filtration module contains a disk rotating around a horizontal axis driven by an electrical motor with adjustable speed. Pressures were measured at the housing periphery and at fluid inlet and outlet by pressure transducers (Validyne DP15).

Rotating disk module

Two different modules (denoted 1 and 2) were built. In both types, a disk (15 cm diameter for module 1 and 14.5 cm for module 2) rotates inside a 15.4-cm ID cylindrical housing around a hollow shaft, through which the retentate is evacuated. A single circular membrane is placed on the front circular plate of the housing opposite the shaft. Several inlet and outlet configurations located either on the back plate or the peripheral wall of the housing were tried. Figure 2a shows the module with the inlet and outlet configuration selected after trials. The first module was machined from Plexiglas, while the second one was made of nylon with enlarged inner channels in order to reduce the pressure drop at the retentate outlet, and therefore the transmembrane pressure. The axial gap between membrane and disk was varied from 3 to 18 mm by using disks of different thicknesses. With these relatively large gaps, the flow field presented an inviscid core rotating at a velocity $k\omega$, where ω is the disk angular velocity and k is the velocity entrainment factor. As was expected, boundary layers developed on the membrane and the disk. The parameter k, which is always < 1, will be determined

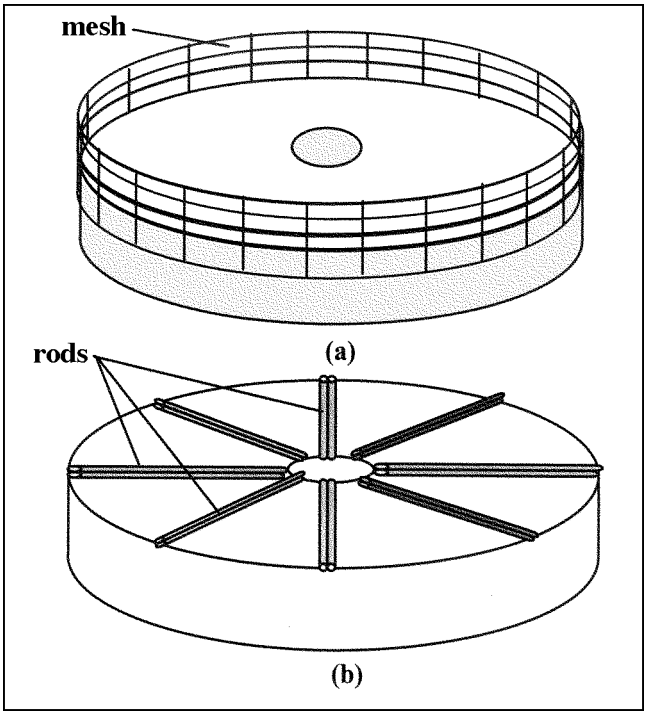

Figure 3. Modified disks equipped with: (a) nylon mesh, (b) eight pairs of 2-mm aluminum rods.

later from pressure measurements inside the housing at different locations and speeds. The local characteristic Reynolds number for the flow near the membrane is defined as

$$Re = k\omega r^2/\nu. \tag{1}$$

In order to raise the coefficient k and increase the shear at the membrane for the same angular velocity of the disk, two modified disks were built. A disk with its edge surrounded by a nylon mesh (Figure 3a) was tried in the Plexiglas module, while an aluminum disk with eight pairs of 2-mm-diameter aluminum rods welded in radial positions was installed in the nylon module (Figure 3b).

These modules were equipped with several flat 16-cm-diameter organic membranes: a symmetric nylon one with a narrow pore distribution centered at 0.2 μm of 6.2×10^{-2} $L\cdot m^{-2}\cdot h^{-1}\cdot Pa^{-1}$ permeability (Ultipor Pall Corp.) and asymmetric PVDF membranes of 0.1 and 0.18 μm (Iris, Orelis, Miribel France) and 2.8×10^{-2} and 4.2×10^{-2} $L\cdot m^{-2}\cdot h^{-1}\cdot Pa^{-1}$ permeability, respectively. The nylon membrane, which was very thin, necessitated a polypropylene grid 0.3 mm thick underneath and was only mounted in the nylon module.

Test fluid

Our test fluid was a suspension of calcium carbonate $CaCO_3$ of specific mass 2,800 $kg\cdot m^{-3}$. Its granulometry was measured by laser diffraction using a Mastersizer X (Malvern Instruments), and the particle size was found to be 0.5 to 18 μm with a mean diameter of 4.7 μm. These particles are resistant to shear, and the particle distribution was found to be unaffected by pumping and circulation inside the filtration module. Therefore the fouling induced by these particles can be considered to be completely external, especially with the nylon membrane, since almost no particles can penetrate inside the pores. These suspensions have been shown by Ziani (1996) to be Newtonian at concentrations below 100 $kg\cdot m^{-3}$ with viscosities at 20°C of 1.3×10^{-3} $Pa\cdot s$ at 10 $kg\cdot m^{-3}$ and of 1.9×10^{-3} $Pa\cdot s$ at 100 $kg\cdot m^{-3}$. At higher concentrations the suspension behaves as pseudoplastic fluid with a viscosity (μ) decreasing when shear (γ) increases according to

$$\mu = 14.5\,\gamma^{-0.225} \quad \text{at } 200\ kg\cdot m^{-3}$$
$$\mu = 163\,\gamma^{-0.537} \quad \text{at } 300\ kg\cdot m^{-3}.$$

Characterization of Flow Inside the Filtration Module

Calculation of shear stress on membrane

These shear stresses are calculated in the boundary layer regime since the ratio s/R is larger than 0.06 in our module. According to Schlichting (1968), the Reynolds number which determines transition to turbulence is Re_d based on disk velocity rather than the Re given by 1.

In the laminar regime ($Re_d < 2.5\times10^5$) we use the similarity solution for the azimuthal velocity induced near a stationary plate by a rotating fluid at infinity proposed by Bödewadt (1940), in which we replace ω by the velocity of the inviscid core $k\omega$.

The velocity field is sought as a similarity solution of the type

$$\text{Radial:} \quad U = rk\omega F(\xi) \tag{2a}$$
$$\text{Azimuthal:} \quad V = rk\omega G(\xi) \tag{2b}$$
$$\text{Axial:} \quad W = (\nu k\omega)^{1/2} H(\xi), \tag{2c}$$

with $\xi = z(k\omega/\nu)^{1/2}$, where z is the axial coordinate normal to the membrane. When Eqs. 2 are substituted into the axisymmetric Navier-Stokes equation ($\partial/\partial\theta = 0$), the system takes the form (Schlichting, 1968, p. 95):

$$F^2 - G^2 + HF' - F'' = 0 \tag{3a}$$
$$2FG + HG' - G'' = 0 \tag{3b}$$
$$2F + H' = 0. \tag{3c}$$

The shear stress at the stationary membrane is given by

$$\tau_{Wl} = \mu\left\|\frac{dV}{dz}\right\|_{Z=0} = \rho r(k\omega)^{3/2}\nu^{1/2}G'(0). \tag{4a}$$

Solving the system of Eqs. 3 with appropriate conditions using the software Mathematica we have obtained $G'(0) = 0.77$, which, using Eq. 4a, gives for the wall shear stress

$$\tau_{Wl} = 0.77\rho\nu^{1/2}(k\omega)^{3/2}r. \tag{4b}$$

It is identical to the expression given by Murkes and Carlsson (1988) and quoted in the Introduction except for the nu-

merical coefficient, which is lower than theirs equal to 1.81. This difference is probably due to the fact that Murkes and Carlsson give the shear stress on the rotating disk, which is larger than the stress on the stationary membrane.

In the turbulent regime ($Re_d > 2.5\times10^5$), the shear stress is estimated from the Blasius friction coefficient for a flat plate (Schlichting, 1968, p. 600)

$$C_F = 0.0592\ Re^{-1/5}, \tag{5}$$

where Re is the local Reynolds number given by Eq. 1. From Eq. 5, the shear stress is expressed as

$$\tau_{Wt} = 0.0296\ \rho\nu^{1/5}(k\omega)^{9/5}r^{8/5}. \tag{6}$$

As in the laminar case, this expression is similar (except it has a lower numerical coefficient) to that (equal to 0.057) given by Murkes and Carlsson (1988) in the turbulent regime, but for the rotating disk surface.

Determination of velocity factor k

The determination was carried out by measuring the pressure in the housing at various radial positions (4.5, 6 and 7.5 cm) by drilling holes in the front plate, in the absence of membrane. The radial pressure gradient in the boundary layer is equal to that in the inviscid core and is given by

$$\frac{\partial p}{\partial r} = \rho r k^2\omega^2. \tag{7}$$

Hence the pressure field is obtained by integration, assuming k is independent of the radius, as was shown by Itoh et al. (1990) and is found to be

$$p = \frac{1}{2}\rho k^2\omega^2 r^2 + p_0, \tag{8}$$

where p_0, the pressure at the center, is also equal to the pressure when the disk is at rest. Pressure data are given in Figure 4a for the first device with a Plexiglas disk in the turbulent regime with a gap of 3 mm at an inlet flow rate of 3.3×10^{-6} $m^3\cdot s^{-1}$. The pressure, p_0, measured at rest was 5,660 Pa. It is seen that the parabolic variation of p with $r\omega$ is well observed for the three radial positions. The value of k, found by regression, varied from 0.305 to 0.34 with a mean of 0.32, which is close to the 0.313 value calculated by Wilson and Schryer (1978) for the two infinite disks. When the Plexiglas disk was replaced by a less polished PVC one, the mean coefficient k rose to 0.35. Since correlation coefficients of the regressions for k were very high and k does not vary much with radial position, we estimate the accuracy of the determination of k to be ±0.01.

Similar pressure measurements were taken on the second device (nylon) with a disk-to-membrane gap of 10 mm at the same inlet flow. Due to reduced pressure loss at the exit, the pressure p_0 was less than in the first module (4,000 Pa). The parabolic pressure distribution with $r\omega$ is again well verified and gives a mean velocity factor of $k = 0.46$ (Figure 4b).

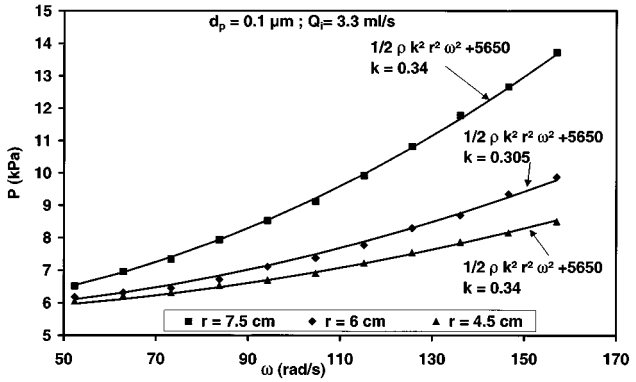

(a)

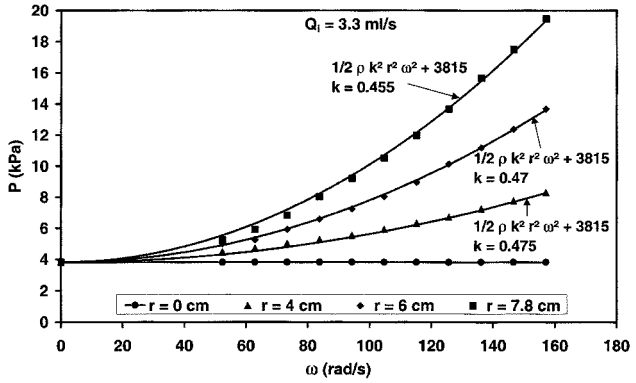

(b)

Figure 4. Determination of velocity coefficient from pressure measurements at various radii for: (a) module 1; (b) module 2.

To confirm these data under filtration conditions, the last experiment was repeated with a 0.2-μm membrane installed and water as a test fluid, and pressure was measured at a tap in the housing lateral wall. The value of k was found to be 0.44 in this case. In order to check the consistency of the filtration data with the pressure distribution of Eq. 8, we calculated the water filtration rate from

$$Q_{FC} = 2\pi L_p\int_0^R pr\,dr = 2\pi L_p\left[\frac{R^2}{2}p_0 + \rho k^2\omega^2\frac{R^4}{8}\right] \tag{9}$$

using the measured membrane water permeability of 6.2×10^{-2} $L\cdot m^{-2}\cdot h^{-1}\cdot Pa^{-1}$. The comparison of calculated and measured filtration flow rates at various rotation speeds is plotted in Figure 5, with $k = 0.44$. The agreement is very close and confirms the validity of Eq. 8 and of the determination of k, which must be independent of radius.

We can now compare the wall shear rates calculated at various radial positions using Eqs. 4 and 6 and $k = 0.46$, with shear rates measured by Rudniak and Wronski (1995) at a fixed membrane in a similar filtration module for disk rotation speeds of 130, 190 and 950 rpm. The agreement is seen in Figure 6 to be very good, confirming the validity of our shear-rate estimation in the module and that k does not

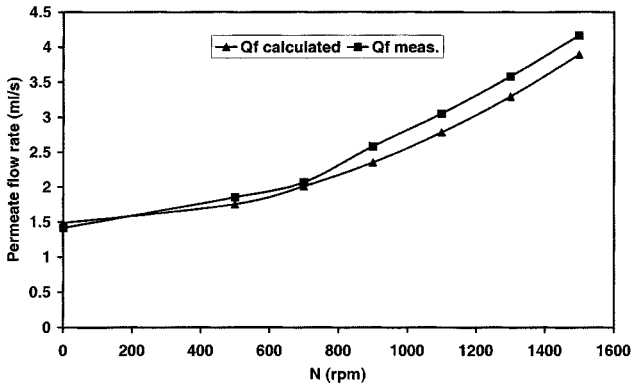

Figure 5. Comparison of measured permeate flux rate in module 2 with the flow rate calculated from Eq. 9.

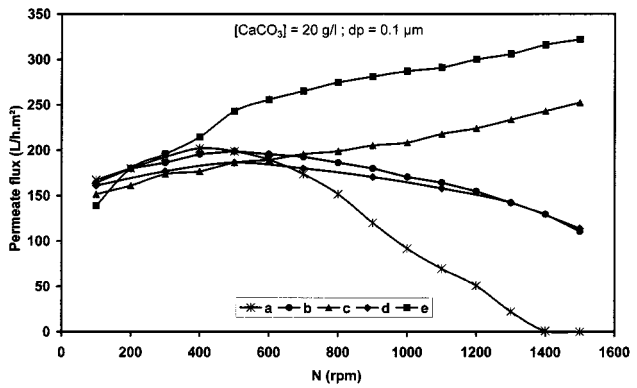

Figure 7. Variations in permeate flux with rotation speed for various inlet and outlet configurations.

change with the flow regime. Since our test fluid has a dynamical viscosity of 1.1×10^{-6} $m^2\cdot s^{-1}$, the flow is laminar at a speed of 1,500 rpm in the central part of the membrane, up to $r = 4.3$ cm and turbulent in the outer ring.

Experimental Results

Effect of inlet/outlet configurations on module performance

The effect of inlet/outlet configurations on module performance was tested on module 1, which was equipped with a 0.1-μm pore membrane, a disk–membrane gap of 3 mm, and a constant $CaCO_3$ concentration of 20 kg·m^{-3}. Five configurations shown in Figure 7 were tested:

(a) Inlet (1) and outlet (2) on housing lateral wall
(b) Inlet (3) and outlet (4) on back plate
(c) Inlet (1) as in (a), and axial outlet (5)
(d) Axial inlet (5), outlet (3) on back plate
(e) Inlet (3), axial outlet (5) [inverse of (d)].

The variations of permeate flux, peripheral pressure, and pressure drop on the module with rotation speed for the various configurations are represented in Figures 7, 8, and 9, respectively. The highest permeate flux is obtained at high speeds with the last configuration (e), and the worst with the first configuration (a).

With the first configuration (a), approximately half of the fluid remains on the right side of the disk and does not come in contact with the membrane. The permeate flux decreases as the angular velocity increases, presumably because the fluid is centrifuged toward the peripheral outlet and the radial velocity along the membrane is reduced.

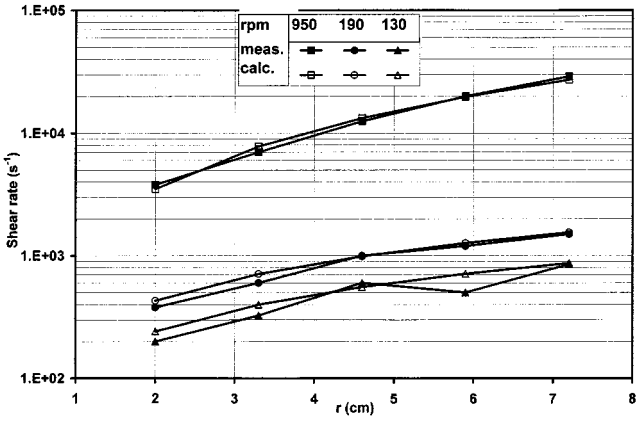

Figure 6. Membrane shear rates measured on module 2 vs. calculated by Rudniak and Wronski (1995) at several radial positions and three rotation speeds.

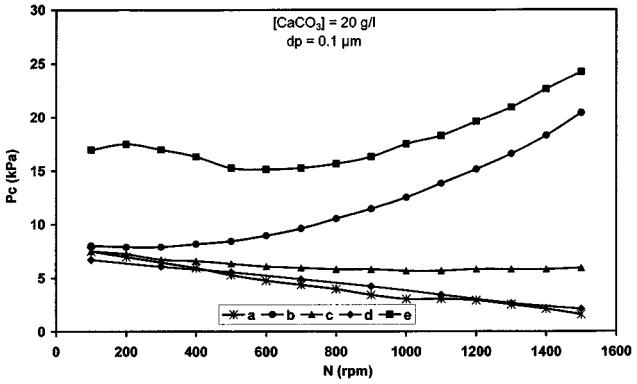

Figure 8. Same as Figure 7 for the peripheral pressure.

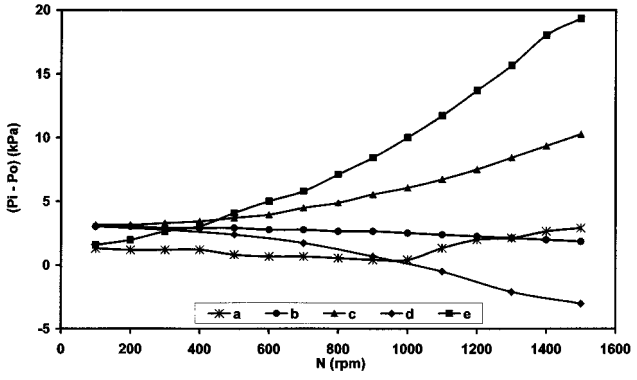

Figure 9. Same as Figure 7 for the pressure drop between module inlet and outlet.

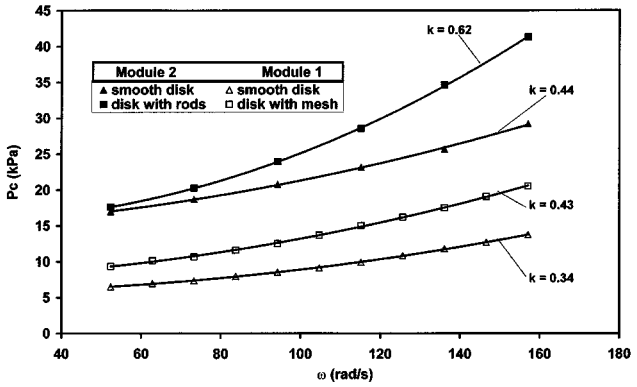

Figure 10. Determination of velocity coefficient *k* for smooth and modified disks, with 10-mm gap.

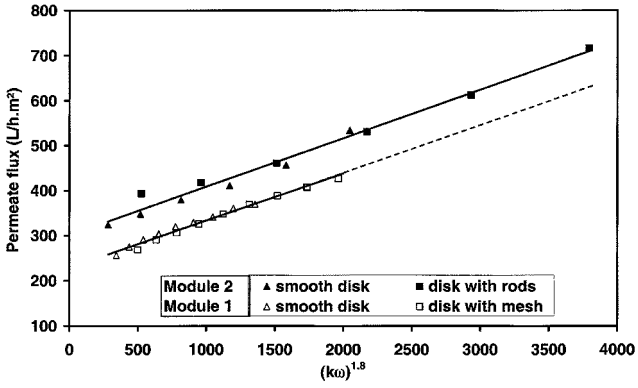

Figure 12. Variation in permeate flux obtained with smooth and modified disks as a function of $(k\omega)^{1.8}$.

In the second configuration ((b), inlet as in Figure 2a), the entering fluid is carried toward the top half of the membrane.

For the third and the fifth configurations, which both have axial outlets, the permeate flux increases continuously at high angular velocities. As seen in Figure 2a, an axial outlet produces an inward radial velocity component as well as recirculation along the membrane. This recirculation pattern has been observed in laminar flow by Szeri et al. (1983), using laser Doppler anemometry. The permeate flux is larger for configuration (e), with the inlet on the back plate, than for configuration (c), with a peripheral inlet, presumably because the peripheral pressure is higher.

Configuration (d) is geometrically similar to the fifth with the flow direction reversed. As seen in Figure 7, the permeate flux drops at high speed, possibly because the fluid is centrifuged away from the membrane compartment without being recirculated.

The variation of pressure drop through the device with rotation speed is seen in Figure 9 to remain constant or to decrease slightly if rotation speed increases, when the outlet is located on the housing (configurations (a), (b) and (d)). Conversely, the pressure drop with an axial outlet (cases (c) and (e)) increases with rotation speed. The reason may be that, since the fluid is centrifuged toward the periphery by the disk, a lower pressure must be applied at high speeds at the exit to suck the fluid out through the shaft, resulting in higher pressure drop. For case (d), the negative pressure drop is due to the centrifugal action of the disk, which sucks the fluid from the axial inlet. This pressure-drop dependence on rotation speed may explain the peripheral pressure variations for various configurations seen in Figure 8. The higher pressure drop for case (e) at high speeds results in a higher peripheral pressure. Conversely, the reduction in pressure drop for cases (a) and (d) may explain the lower peripheral pressures at high speeds.

We have therefore retained configuration (e), which yields the highest permeate flux at high speed and the highest peripheral pressure. It also yields the highest pressure drop, but since the pressure drop remains under 20 kPa at 1,500 rpm, it is acceptable.

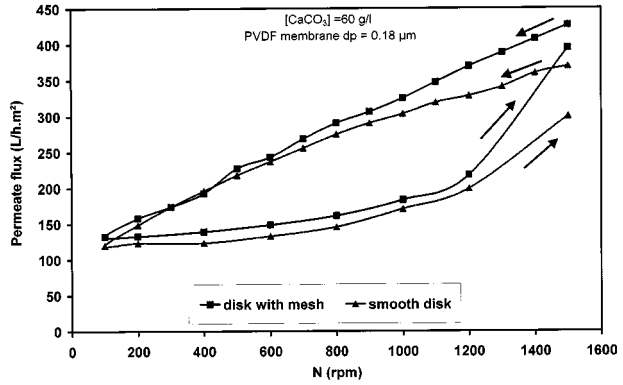

Figure 11. Variation in permeate flux during a velocity cycle 1,500–500–1,500 rpm with a smooth disk and a disk equipped with a mesh in module 1; arrows show the variation sequence.

Effect of disk modification on permeate flux

The purpose of surrounding the disk with a nylon mesh was to carry the disk momentum into the core fluid layer, in order to raise the velocity factor k. Figure 10 shows the determination of k in module 1 from pressure measurements at three radial positions for a Plexiglas disk equipped with a mesh ring. The coefficient was raised from 0.32 to 0.42. The consequence on the variation of permeate flux with rotation using a $CaCO_3$ suspension of 60 $kg \cdot m^{-3}$ and a PVDF membrane of 0.18 μm is illustrated in Figure 11. The gain is seen to be larger above 1,300 rpm. In fact, this gain can be shown to be exactly due to the increase in coefficient k, as shown in Figure 12, since the data for the normal and modified disks fall on the same straight lines when plotted as a function of $(k\omega)^{1.8}$. We have chosen this representation, which corresponds to the variation of wall shear stress with $k\omega$ given by Eq. 6. In fact, Figure 12 also shows that the permeate flux is indeed proportional to the wall shear stress.

The effect of radial rods, welded to a disk to form small vanes, on the velocity coefficient k is also illustrated in Figure 10 for a test in module 2. In that case k was increased from 0.44 to 0.62. According to Murkes and Carlsson (1988),

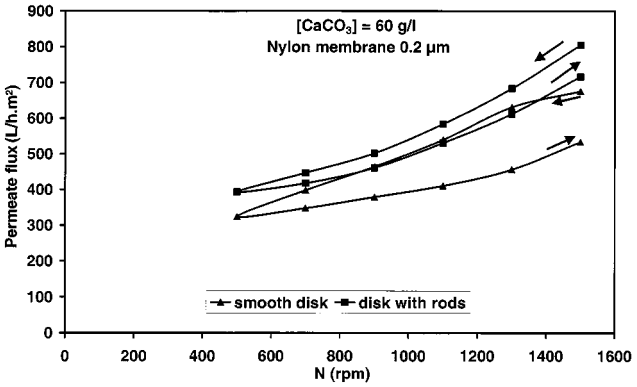

Figure 13. Variation in permeate flux during a velocity cycle 1,500–500–1,500 rpm with a smooth disk and a disk equipped with rods in module 2, showing the decrease in fouling due to the modified disk; arrows show the variation sequence.

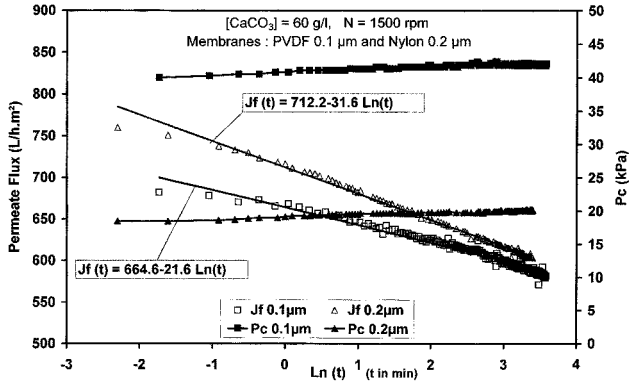

Figure 15. Variation in permeate flux and peripheral pressure with time in semilogarithmic coordinates for nylon and PVDF membranes, in module 2.

Schiele (1978) has reported a velocity coefficient of 0.9 with a disk equipped with eight radial vanes and a small axial gap such that the inviscid core disappears. The variation in permeate flux during a rotation velocity cycle is represented in Figure 13. The increase in permeate flux is important, especially when the speed is increased again, showing that the fouling formation induced by the slowing down of the disk is reduced by the presence of rods. As in the case of the mesh, the increase in permeate flux is exactly due to the increase in the coefficient k, and the permeate flux is then proportional to the wall shear stress (Figure 12).

The reduction of fouling due to the rods is confirmed by photographs of the membrane (Figure 14) taken after filtration during a velocity cycle from 1,500 to 500 rpm, as in Figure 13, and rinsing it with water. Without rods, the membrane is covered by a cake a few millimeters thick, presenting a spiral pattern due to fluid instabilities. Conversely, there is no visible cake when the disk is equipped with rods.

The permeate flux was found to decrease by 7% when the axial gap was increased from 5 to 18 mm at 1,500 rpm and a peripheral pressure of 40 kPa.

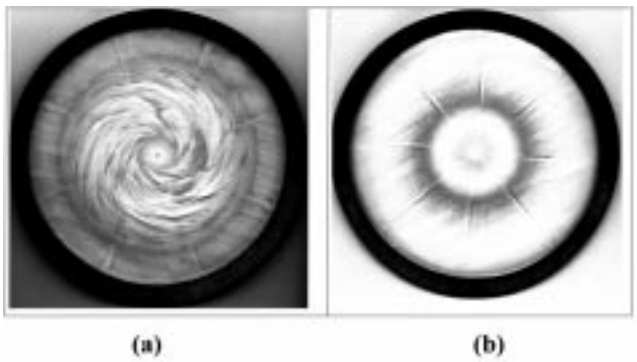

Figure 14. Membranes after filtration and rinsing with water: (a) with a smooth disk; (b) when using a disk equipped with rods.

Variation of permeate flux with time under constant conditions

The variation of permeate flux and peripheral pressure with time in the laminar regime (400 rpm) is represented in Figure 15 for a concentration of 60 $kg \cdot m^{-3}$. It is seen that the permeate flux decays exponentially with time to a constant level reached after about 10 min, while the peripheral pressure rises slightly to a constant level. When the flow becomes turbulent at a higher speed (1,500 rpm), the permeate flux decays continuously with time according to a logarithmic law (Figure 15). As expected the permeate flux is larger for the 0.2-μm pore membrane than for the 0.1-μm one, but even with the small pore membrane, the flux remains very high, in excess of 570 $L \cdot h^{-1} \cdot m^{-2}$. Bouzerar et al. (1998) have filtrated $CaCO_3$ suspensions at concentrations of up to 700 $kg \cdot m^{-3}$, obtaining 200 $L \cdot h^{-1} \cdot m^{-2}$ at 2,000 rpm and a peripheral pressure of 60 kPa.

Discussion and Conclusion

The geometrical configuration and the internal fluid circulation inside the module have a marked effect on the filtration performance. The choice of a retentate outlet through the shaft gave the best result and, in addition, had the advantage of cooling the shaft, which is heated by friction. We have also proposed and validated a simple method for determining the core-velocity factor k using measurements of peripheral pressure as a function of rotation speed. We have found that this coefficient did not vary with the radius or with the flow regime. Although it could not be verified with high accuracy, this coefficient did not seem to vary with speed, at least until 2,000 rpm.

The coefficient k may also be a good criterion of module efficiency, since a higher value of k will produce a higher permeate flux at the same speed than another module with a smaller value of k. Of course, when we increase k in our device by welding rods on the disk, we can expect that the torque necessary to rotate the disk is increased in proportion to the increase in shear rate. But it is possible to show by simple qualitative reasoning that the energy necessary per unit volume of permeate was most probably reduced with the

modified disk. We have shown in Figure 12 that the permeate flux is a function of $(k\omega)^{1.8}$ and membrane shear stress. Thus, if two modules that have the same membrane shear stress yield the same permeate flux, the module with the higher coefficient k will have a smaller disk angular velocity ω. The power required to drive the disk is $C\omega$, where the torque C is a function of shear-stress distribution on the disk. Consequently, the module with the highest k will require the lowest energy for driving the disk. The specific energy (per m^3 of permeate) will be independent of k, since both the permeate flux and the power to drive the disk are proportional to the shear stress. Concerning the effect of angular velocity, we will have the same situation as with conventional cross-flow filtration, namely that the specific energy consumption is proportional to ω, while the membrane area required decreases with increasing angular velocity. This situation leads to the existence of an optimal angular velocity that minimizes the total cost (investment + energetic costs).

The axial gap between disk and membrane had almost no effect on the permeate flux when it varied from 4 to 18 mm, which is logical, since increasing the gap only increases the thickness of the inviscid core without changing the shear stress on the membrane. But it is legitimate to ask whether the permeate flux would be increased if the device was operated in the completely viscous regime, which occurs when the gap is narrow ($s/R < 0.05$). This regime starts to appear at the disk top when $s \leq 3.5$ mm, and prevails on the major part of the membrane for $s \leq 2$ mm. According to Murkes and Carlsson (1988), the shear stress in the turbulent narrow gap regime is given by

$$\tau'_{wt} = 0.008\,\rho(\omega r)^{7/4}\left(\frac{\nu}{s}\right)^{1/4}. \qquad (10)$$

Since this flow was of the Couette type, the shear stress is the same on the disk and on the membrane. By dividing Eq. 6 by Eq. 10, we obtain

$$X = \frac{\tau_{wt}}{\tau'_{wt}} = 3.7k^{7/4}Re^{1/20}\left(\frac{s}{r}\right)^{1/4}. \qquad (11)$$

For a rotation speed of 1,500 rpm, a disk radius of 7.25 cm and $k = 0.45$, the Reynolds number is 3.3×10^5 and the ratio X is found to be 0.72 for $s = 3.5$ mm. Thus if Eq. 10 is correct, a narrow gap would yield a higher permeate flux, but would increase the risk of friction between the disk and the cake formed in the central part of the membrane in the case of highly charged fluids. Another risk is the possibility of the disk damaging the membrane if a part of the membrane is being sucked toward the disk by low pressure. For these reasons, operation in the fully viscous regime seems to be possible only for large disk diameters of at least 30 cm.

We feel that the device presented in this article has an important potential for further development by increasing the rotation speed and by optimizing the disk shape. For instance, the data of Frenander and Jönsson (1996) show that the permeate flux continues to increase at high disk peripheral velocities of up to 20 m/s. This device proved itself in our laboratory to be very effective for filtering various suspensions, such as ferric hydroxide suspensions in saline medium (Bouzerar et al., 2000) and fermentation broths (Harscoat et al., 1999). Ferric hydroxide concentrations of 130 g/L were reached, while it was not possible to exceed 45 g/L with conventional cross-flow filtration.

Acknowledgments

The support of the Regional Council of Picardy is acknowledged.

Notation

J_f = permeate flux (L/hm^2)
L_p = membrane permeability ($L\cdot h^{-1}\cdot m^{-2}\cdot Pa^{-1}$)
N = rotation speed (rpm)
p_c = peripheral pressure (Pa)
r = radial distance (m)
R = disk radius (m)
s = gap between disk and membrane (m)
T = temperature (°C)

Greek letters

γ_w = wall (s^{-1})
ν = kinematic viscosity (m^2/s)
ρ = fluid density (kg/m^3)
τ_w = wall shear stress (Pa) (subscript l: laminar, t: turbulent)

Literature Cited

Beaudoin, G., and M. Y. Jaffrin, "Plasma Filtration in Couette Flow Membrane Device," *Artif. Organs*, **13**, 43 (1989).
Bödewadt, U. T., "Die Drehströmung über Feste Grunde- Z. Angew," *Math. Mech.*, **20**, 241 (1940).
Bouzerar, R., M. Y. Jaffrin, and L. H. Ding, "Dynamic Crossflow Filtration of Mineral Suspensions at High Concentration Using a Rotating Disc," AIChE Meeting, Miami, FL (1998).
Bouzerar, R., M. Y. Jaffrin, A. Lefevre, and L. Ding, "Concentration of Ferric Hydroxide Suspensions in Saline Medium by Dynamic Cross-Flow Filtration," *J. Memb. Sci.*, **165**(1), 111 (2000).
Dal-Cin, M. M., C. N. Lick, A. Kumar, and S. Lealess, "Dispersed Phase Back Transport During Ultrafiltration of Cutting Oil Emulsions with a Spinning Disc Geometry," *J. Memb. Sci.*, **141**, 165 (1998).
Frenander, U., and A. S. Jönsson, "Cell Harvesting by Cross-Flow Microfiltration Using a Shear-Enhanced Module," *Biotechnol. Bioeng.*, **52**, 397 (1996).
Harscoat, C., M. Y. Jaffrin, R. Bouzerar, and J. Courtois, "Influence of Fermentation Conditions and Microfiltration Process on Membrane Fouling During Recovery of Glucuronane Polysaccharides from Fermentation Broths," *Biotechnol. Bioeng.*, **65**, 500 (1999).
Itoh, M., Y. Yamada, S. Imao, and M. Gonda, "Experiment on Turbulent Flow Due to an Enclosed Rotating Disk," *Engineering, Turbulence Modeling and Experiments*, Elsevier, Amsterdam (1990).
Jönsson, A. S., "Influence of Shear Rate on the Flux During Ultrafiltration of Colloidal Substances," *J. Memb. Sci.*, **79**, 93 (1993).
Lee, S., A. Burt, G. Russoti, and B. Buckland, "Microfiltration of Recombinant Yeast Cells Using a Rotating Disk Dynamic Filtration System," *Biotechnol. Bioeng.*, **48**, 386 (1995).
Lopez-Leiva, A. M., "Ultrafiltration at Low Degrees of Concentration Polarization: Technical Possibilities," *Desalination*, **35**, 115 (1980).
Meyer, F., I. Gehmlich, R. Guthke, A. Gorak, and W. A. Knorre, "Analysis and Simulation of Complex Interactions During Dynamic Microfiltration of Escherichia coli Suspensions," *Biotechnol. Bioeng.*, **59**, 189 (1998).
Murkes, J., and C. G. Carlsson, *Crossflow Filtration*, Wiley, New York (1988).
Nuortila-Jokinen, J., and M. Nyström, "Comparison of Membrane Separation Processes in the Internal Purification of Paper Mill Water," *J. Memb. Sci.*, **119**, 99 (1996).

Pessoa, A., and M. Vitolo, ''Evaluation of Cross-Flow Microfiltration Membranes Using a Rotary Disc-Filter,'' *Process Biochem.*, **33**, 39 (1998).
Rudniak, L., and S. Wronski, ''Influence of Hydrodynamics of Rotary Dynamic Filters on Separation Processes,'' *Chem. Eng. Technol.*, **18**, 90 (1995).
Schiele, B., ''Untersuchungen zur Filtration Feindisperser Suspensionen im Dynamischen Druckfilter,'' PhD Thesis, Universität Stuttgart, Stuttgart, Germany (1978).
Schlichting, H., *Boundary Layer Theory*, 7th ed., McGraw-Hill, New York (1968).
Szeri, A. Z., S. J. Schneider, F. Labbe, and H. N. Kaufman, ''Flow Between Rotating Disks. Part 1. Basic Flow,'' *J. Fluid Mech.*, **134**, 103 (1983).
Wilson, L. O., and N. L. Schryer, ''Flow Between a Stationary and a Rotating Disc with Suction,'' *J. Fluid Mech.*, **85**, 479 (1978).
Ziani, Y., ''Etude de la Formation et du Réentraînement d'un Dépôt lors de la Filtration Dynamique d'une Suspension Minérale,'' PhD Thesis, Univ. of Technology of Compiègne, Compiègne, France (1996).

Manuscript received July 12, 1999, and revision received Oct. 13, 1999.